The Plant Cell, Vol. 30: 466–480, February 2018, www.plantcell.org © 2018 ASPB.

A Role for MINIYO and QUATRE-QUART2 in the Assembly of RNA Polymerases II, IV, and V in Arabidopsis

Yaoxi Li,[a,b,c,1] Yuxiang Yuan,[a,d,1] Xiaofeng Fang,[a,e,1] Xiuli Lu,[a] Bi Lian,[a,e] Gaozhan Zhao,[a,e] and Yijun Qi[a,b,e,2]

[a] Center for Plant Biology, School of Life Sciences, Tsinghua University, Beijing 100084, China
[b] Graduate Program, Chinese Academy of Medical Sciences and Peking Union Medical College, Beijing 100730, China
[c] National Institute of Biological Sciences, Beijing 102206, China
[d] Peking University-Tsinghua University-National Institute of Biological Sciences Joint Graduate Program, Tsinghua University, Beijing 100084, China
[e] Tsinghua-Peking Center for Life Sciences, Beijing 100084, China

ORCID ID: 0000-0002-7100-1700 (Y.Q.)

RNA polymerases IV and V (Pol IV and Pol V) are required for the generation of noncoding RNAs in RNA-directed DNA methylation (RdDM). Their subunit compositions resemble that of Pol II. The mechanism and accessory factors involved in their assembly remain largely unknown. In this study, we identified mutant alleles of *MINIYO* (*IYO*), *QUATRE-QUART2* (*QQT2*), and *NUCLEAR RNA POLYMERASE B11/D11/E11* (*NRPB/D/E11*) that cause defects in RdDM in *Arabidopsis thaliana*. We found that Pol IV-dependent small interfering RNAs and Pol V-dependent transcripts were greatly reduced in the mutants. NRPE1, the largest subunit of Pol V, failed to associate with other Pol V subunits in the *iyo* and *qqt2* mutants, suggesting the involvement of IYO and QQT2 in Pol V assembly. In addition, we found that IYO and QQT2 were mutually dependent for their association with the NRPE3 subassembly prior to the assembly of Pol V holoenzyme. Finally, we show that IYO and QQT2 are similarly required for the assembly of Pol II and Pol IV. Our findings reveal IYO and QQT2 as cofactors for the assembly of Pol II, Pol IV, and Pol V and provide mechanistic insights into how RNA polymerases are assembled in plants.

INTRODUCTION

DNA methylation is an important epigenetic mechanism that regulates gene expression, silences transposable elements, and safeguards genome stability. In *Arabidopsis thaliana*, DNA methylation occurring in all CG, CHG, and CHH sequence contexts (H represents either A, T, or C) can be established through an RNA-directed DNA methylation (RdDM) pathway (Matzke et al., 2009; Law and Jacobsen, 2010).

RdDM entails two plant-specific RNA polymerases, RNA polymerase IV (Pol IV) and Pol V, which generate 24-nucleotide small interfering RNAs (siRNAs) (Herr et al., 2005; Kanno et al., 2005; Onodera et al., 2005) and long intergenic noncoding (IGN) RNAs, respectively (Wierzbicki et al., 2008). Pol IV-dependent siRNAs are primarily incorporated into ARGONAUTE4 (AGO4) in the cytoplasm and then reenter the nucleus (Ye et al., 2012), where Pol V-dependent IGN scaffold transcripts recruit siRNA/AGO4 complexes and DOMAIN REARRANGED METHYTRANSFERASE2 (DRM2) to target loci to direct DNA methylation (Wierzbicki et al., 2009; Zhong et al., 2014). Pol V can also regulate siRNA biogenesis, likely through a feedback regulation between DNA methylation and siRNA production (Pontier et al., 2005; Li et al., 2006).

The subunit compositions of Pol IV and Pol V largely resemble that of Pol II, which mainly transcribes mRNAs and microRNAs (miRNAs) (Ream et al., 2009; Law et al., 2011). In Arabidopsis, Pol II also transcribes long scaffold IGN transcripts, which assist the recruitment of Pol IV and Pol V to RdDM-targeted loci (Zheng et al., 2009). Pol IV, Pol V, and Pol II each consist of 12 subunits, which are termed NUCLEAR RNA POLYMERASE D (NRPD), NRPE, and NRPB (RPB in yeast and human cells) subunits, respectively (Ream et al., 2009; Law et al., 2011). Although Pol IV and Pol V have unique catalytic subunits (NRPD1, NRPE1, and shared NRPD/E2) compared with Pol II (NRPB1 and NRPB2), many other Pol IV and Pol V subunits have identical counterparts in Pol II, indicating that Pol IV and Pol V evolved from Pol II (Ream et al., 2009; Tucker et al., 2010; Wang and Ma, 2015).

Our current understanding of the assembly of RNA polymerases comes from studies of Pol II in yeast and humans, which revealed that the formation of a RPB3/RPB11 heterodimer initiates the assembly (Kolodziej and Young, 1991; Kimura et al., 1997). RPB10 and RPB12 associate with the RPB3/RPB11 heterodimer to form a RPB3 subassembly, which is subsequently bound by a RPB2 subassembly comprising RPB2 and RPB9 and a RPB1 subassembly including RPB1, RPB5, RPB6, and RPB8. Finally, a RPB4/RPB7 subassembly attaches to the 10-subunit core enzyme (Wild and Cramer, 2012). RPAP1, RPAP2, GrinL1a, GPN1, GPN2, and GPN3 were identified to be Pol II assembly factors that associate with the RPB3 subassembly, whereas RPAP3 (hSpagh) and the R2TP/Prefoldin-like complex bind and stabilize the RPB1 subassembly (Boulon et al., 2010). The process of Pol II assembly takes place in the cytoplasm and the Pol II-specific import factor Iwr1 moves completely assembled Pol II into the nucleus (Czeko et al., 2011). How plant Pol II as well as Pol IV and Pol V are assembled remains largely unknown.

In this study, we isolated viable point mutant alleles of *MINIYO* (*IYO*) (Sanmartín et al., 2011), *QUATRE-QUART2* (*QQT2*) (Lahmy

[1] These authors contributed equally to this work.
[2] Address correspondence to qiyijun@tsinghua.edu.cn.
The author responsible for distribution of materials integral to the findings presented in this article in accordance with the policy described in the Instructions for Authors (www.plantcell.org) is: Yijun Qi (qiyijun@tsinghua.edu.cn).
www.plantcell.org/cgi/doi/10.1105/tpc.17.00380

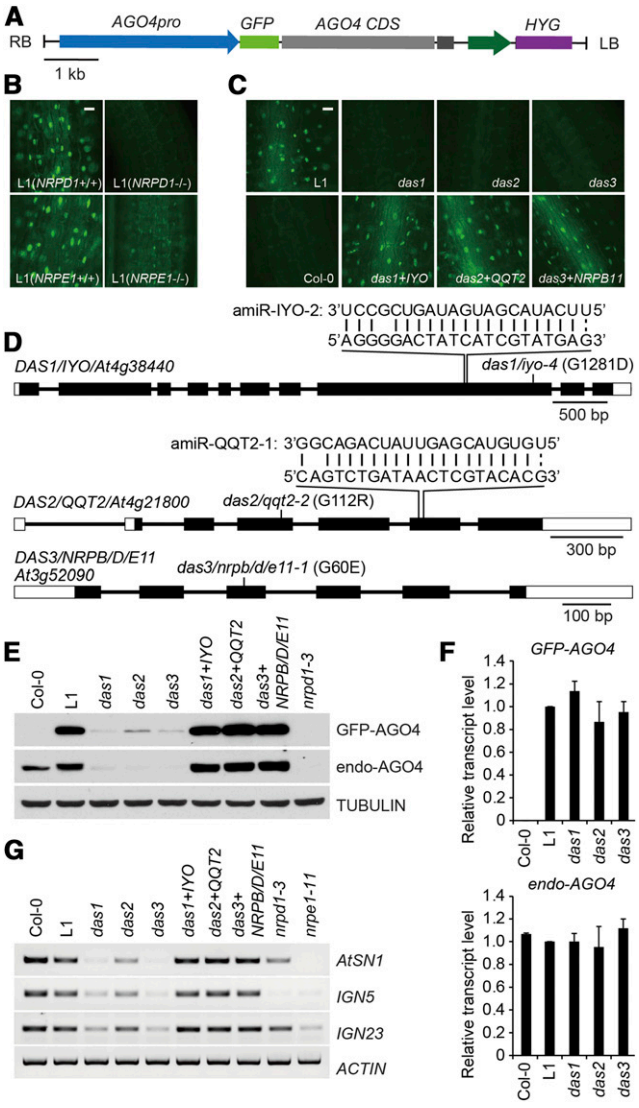

Figure 1. Identification and Characterization of the *das* Mutants.

(A) Schematic of *pAGO4:GFP-AGO4* construct for screening for the *das* mutants.

(B) Representative images showing the expression of GFP-AGO4 in hypocotyl cells of 7-d-old seedlings in the indicated genetic background. Bar = 20 μm.

(C) Representative images showing the expression of GFP-AGO4 in three *das* mutants and the *das* mutants complemented with *IYO*, *QQT2*, and *NRPB/D/E11* sequences, respectively. Bar = 20 μm.

(D) Schematic diagram showing the gene structures of *DAS1/IYO* (*At4g38440*), *DAS2/QQT2* (*At4g21800*), and *DAS3/NRPB/D/E11* (*At3g52090*). The positions of the mutations and amiRNA-targeting sites are indicated. The black boxes and horizontal lines represent exons and introns, respectively, and the white boxes represent untranslated regions.

(E) Detection of GFP-AGO4 and endogenous AGO4 proteins in the indicated plants by immunoblot analysis. TUBULIN was detected as a loading control.

(F) Detection of *GFP-AGO4* and *endogenous AGO4* (*endo-AGO4*) transcripts in the indicated plants by quantitative RT-PCR analysis. Error bars represent SD from the mean value of three biological replicates (one biological replicate means one independent experiment with two technical replicates). Student's *t* tests were applied, but no significant difference ($P < 0.05$) was detected between L1 and the *das* mutants.

(G) Chop-PCR analysis of DNA methylation levels at *AtSN1*, *IGN5*, and *IGN23* in the indicated plants. A fragment of AC*TIN* that lacks *Hae*III site was amplified as a control.

et al., 2007), and *NUCLEAR RNA POLYMERASE B11/D11/E11* (*NRPB/D/E11*) in a forward genetic screen designed to identify RdDM pathway components. The accumulation of 24-nucleotide siRNAs and IGN transcripts, as well as DNA methylation, especially in CHG and CHH contexts, were severely compromised in these mutants, suggesting impaired Pol IV and Pol V activities. We further found that IYO and QQT2 associated with the NRPE3 subassembly to assist the assembly of Pol V holoenzyme. Finally, we found that IYO and QQT2 are also required for the assembly of Pol II and Pol IV. Our study thus provides insights into the mechanism of the assembly of RNA polymerases in plants.

RESULTS

A Forward Genetic Screen Identifies IYO, QQT2, and NRPB/D/E11 as Components in the Arabidopsis RdDM Pathway

AGO4 requires siRNA loading to become stable (Li et al., 2006). Thus, a screen for mutants defective in AGO4 stability would allow us to identify components required for siRNA accumulation. We used an Arabidopsis transgenic line expressing N-terminally GFP-tagged AGO4 (GFP-AGO4) under the control of the native *AGO4* promoter (L1) (Figure 1A) (Ye et al., 2012) for such screen. The efficacy of this screen was validated by introducing the *nrpd1-3* or *nrpe1-11* mutation into L1. The mutations did not affect the transcription of *GFP-AGO4* transgene (Supplemental Figure 1A) but led to nearly eliminated or reduced accumulation of GFP-AGO4 protein (Figure 1B; Supplemental Figure 1B).

Based on the reduction in GFP-AGO4 level and DNA methylation at three representative RdDM target loci (*AtSN1*, *IGN5*, and *IGN23*), we identified 68 *das* (for *defective in AGO4 stability*) mutants. These include 65 new mutant alleles of known RdDM pathway genes and three mutants that harbor mutations in genes without known RdDM-related functions, *das1*, *das2*, and *das3* (Figure 1C; Supplemental Table 1). In *das1*, a point mutation (G4756A) occurred in the *IYO* gene (*At4g38440*) changes Gly-1281 to Asp; in *das2*, a point mutation (G1108A) in the *QQT2* gene (*At4g21800*) converts Gly-112 to Arg; whereas in *das3*, a point mutation (G474A) in the *NRPB/D/E11* gene (*At3g52090*) results in a Gly-60-to-Glu change (Figure 1D). Immunoblot analyses revealed that the protein levels of GFP-AGO4 and endogenous AGO4 were dramatically decreased in all three mutants (Figure 1E). However, their corresponding transcript levels remained unaltered (Figure 1F; Supplemental File 1), suggesting that the mutations impair AGO4 stability. The DNA methylation levels at *AtSN1*, *IGN5*, and *IGN23*, were greatly reduced in these three mutants, as determined by Chop-PCR analysis (Figure 1G), indicating that the mutations affect RdDM. Transformation of *das1*, *das2*, and *das3* with the respective *IYO*, *QQT2*, and *NRPB/D/E11*

full genomic sequences restored GFP-AGO4 and endogenous AGO4 accumulation and DNA methylation at selected loci (Figures 1C, 1E, and 1G), indicating that the mutations of *IYO*, *QQT2*, and *NRPB/D/E11* are responsible for the reduction of AGO4 protein and DNA hypomethylation in *das1*, *das2*, and *das3*, respectively. Accordingly, *das1*, *das2*, and *das3* were renamed *iyo-4*, *qqt2-2*, and *nrpb/d/e11-1*, respectively.

IYO encodes a positive regulator of transcription elongation that is essential for the onset of cell differentiation (Sanmartín et al., 2011; Muñoz et al., 2017), and *QQT2* encodes an ATP/GTP binding protein that regulates embryogenesis (Lahmy et al., 2007). *NRPB/D/E11* encodes a noncatalytic subunit common to Pol II, Pol IV, and Pol V (Ream et al., 2009; Law et al., 2011). However, the *iyo-4*, *qqt2-2*, and *nrpb/d/e11-1* mutants that carry point mutations did not exhibit developmental defects (Supplemental Figure 2A). To further confirm that *IYO* and *QQT2* are indeed involved in the RdDM pathway, we generated lines overexpressing artificial miRNAs (amiRNAs) targeting *IYO* and *QQT2* (amiR-IYO and amiR-QQT2), respectively (Supplemental Figures 2B to 2D and Supplemental File 1). As expected, the DNA methylation levels at *AtSN1* and *IGN5* were markedly decreased in these amiRNA lines (Supplemental Figure 2E), confirming that *IYO* and *QQT2* are RdDM pathway components. It is noteworthy that all amiRNA lines displayed obvious developmental phenotypes (Supplemental Figure 2B), consistent with the fact that *IYO* and *QQT2* are essential for plant development (Lahmy et al., 2007; Sanmartín et al., 2011).

Mutations in *IYO*, *QQT2*, and *NRPB/D/E11* Impair Global DNA Methylation

To quantitatively measure the change of DNA methylation levels at RdDM loci, we performed locus-specific bisulfite sequencing and found that the CG, CHG, and CHH methylation levels at *AtSN1* and *IGN5* were substantially decreased in all three *iyo-4*, *qqt2-2*, and *nrpb/d/e11-1* mutants (Figure 2A). At *IGN23*, the CG methylation levels in the *iyo-4*, *qqt2-2*, and *nrpb/d/e11-1* mutants remained comparable to that in L1, whereas the CHG and CHH methylation levels were decreased (Figure 2A). To investigate the effects of *iyo*, *qqt2*, and *nrpb/d/e11-1* mutations on the Arabidopsis DNA methylome, we performed whole-genome bisulfite sequencing. Similar to *nrpd1-3* and *nrpe1-11*, the *iyo-4* and *nrpb/d/e11-1* mutations led to mildly, moderately, and severely compromised CG, CHG, and CHH methylation, respectively (Figure 2B; Supplemental File 1). The *qqt2-2* mutation also resulted in decreased methylation in each sequence context, but to a lesser extent when compared with *iyo-4* and *nrpb/d/e11-1* (Figure 2B; Supplemental File 1).

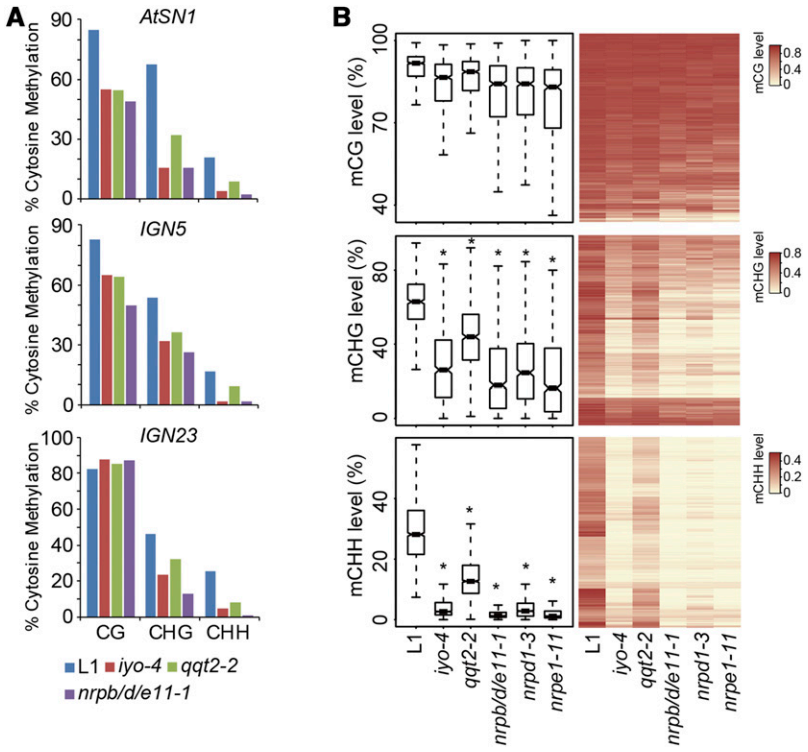

Figure 2. Effects of the *iyo-4*, *qqt2-2*, and *nrpb/d/e11* Mutations on DNA Methylation.

(A) Detection of DNA methylation at *AtSN1*, *IGN5*, and *IGN23* in L1 and the indicated mutants by locus-specific bisulfite sequencing. The overall percentage of methylated cytosines in different sequence contexts is presented. More than 20 clones were sequenced for each sample.

(B) Box plots (panels on the left) and heat maps (panels on the right) of CG, CHG, and CHH methylation levels at RdDM loci in the indicated plants determined by whole-genome bisulfite sequencing. Asterisks indicate a significant difference between L1 and the mutants ($P < 10^{-15}$, Mann-Whitney U test).

IYO, QQT2, and NRPB/D/E11 Are Required for the Production of Pol IV-Dependent 24-Nucleotide siRNA and Pol V-Dependent Transcripts

The destabilization of AGO4 in the *iyo-4*, *qqt2-2*, and *nrpb/d/e11-1* mutants suggest that IYO, QQT2, and NRPB/D/E11 may regulate siRNA production. To test this, we performed small RNA deep sequencing analysis. Our results showed that the abundance of 24-nucleotide siRNAs in all three mutants was significantly lower than that in L1 (Figure 3A; Supplemental File 1). In *iyo-4* and *nrpb/d/e11-1*, the 24-nucleotide siRNA levels were nearly undetectable, similar to that in *nrpd1-3* (Figure 3A; Supplemental File 1). To validate these results, we detected siRNAs generated from representative loci *siR1003*, *AtRep2*, and *SimpleHAT2* by small RNA gel blot. Consistently, we found that the accumulation of siRNAs from these loci was abolished in all three mutants (Figure 3B). The *IYO*, *QQT2*, and *NRPB/D/E11* transgenes fully rescued the defects of *iyo-4*, *qqt2-2*, and *nrpb/d/e11-1* in accumulating siRNAs, respectively (Figure 3B), suggesting that IYO, QQT2, and NRPB/D/E11 regulate siRNA production. We further analyzed the extent to which IYO-, QQT2-, or NRPB/D/E11-dependent siRNA-generating loci overlap with Pol IV- or Pol V-dependent loci. Strikingly, IYO- or NRPB/D/E11-dependent loci almost completely overlapped with Pol IV- and Pol V-dependent loci, whereas over half of Pol IV-dependent loci and the majority of Pol V-targeted loci were QQT2 dependent (Figure 3C). We also analyzed the extent to which IYO- and QQT2-dependent siRNA-generating loci overlap. QQT2-dependent siRNA loci were almost all dependent on IYO. However, a subset of IYO-dependent loci was QQT2-independent (Figure 3C)

Next, we examined whether IYO, QQT2, and NRPB/D/E11 are required for the production of Pol V-dependent *IGN* transcripts. We performed RT-PCR to detect changes in the level of *IGN* transcripts in the mutants. We found that the levels of *IGN* transcripts produced from *AtSN1*, *IGN5*, and *IGN6* were all markedly decreased (Figure 3D).

These data together indicate that *IYO*, *QQT2*, and *NRPB/D/E11* are required for the production of Pol IV-dependent siRNAs and Pol V transcripts.

IYO and QQT2 Are Required for Pol V Assembly

IYO shows sequence similarity to the yeast Ydr527wp protein (also named RBA50) and human RPAP1 (Jeronimo et al., 2004; Sanmartín et al., 2011). Whereas Ydr527wp associates with RPB2, RPB3, and RPB11 subunits critical for yeast Pol II assembly

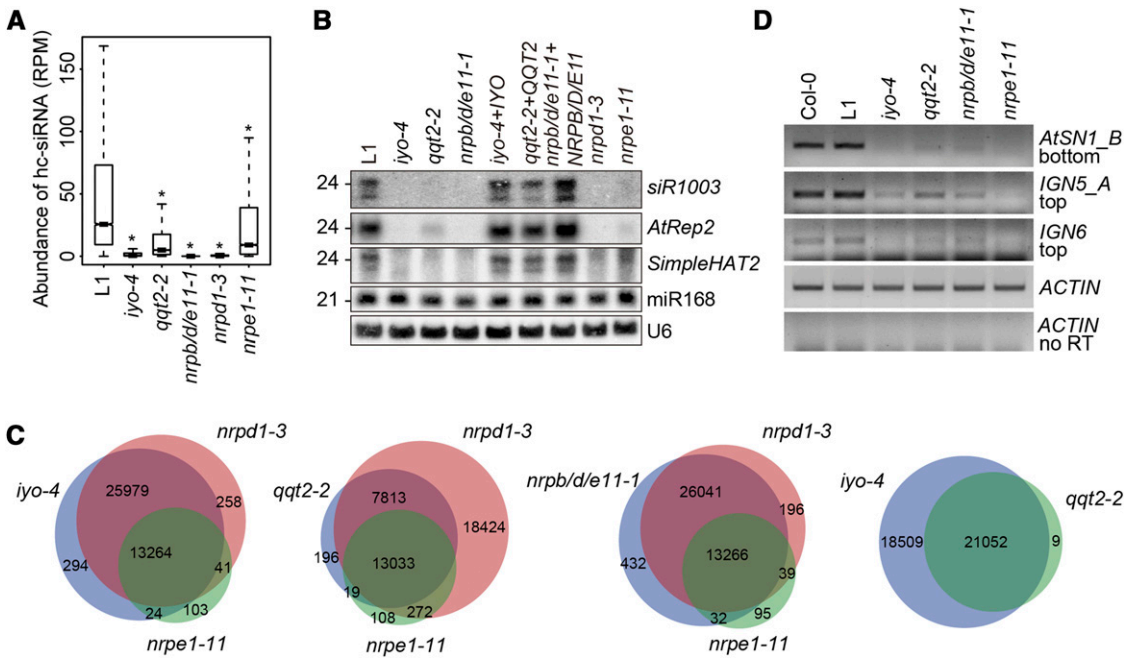

Figure 3. Effects of the *iyo-4*, *qqt2-2*, and *nrpb/d/e11* Mutations on the Production of Pol IV-Dependent 24-Nucleotide siRNA and Pol V-Dependent Transcripts.

(A) Box plots showing the levels of 24-nucleotide siRNAs in the indicated plants as measured by small RNA deep sequencing. Asterisks indicate a significant difference between Col-0 and the mutants ($P < 10^{-15}$, Mann-Whitney U test).

(B) Detection of siRNA production at selected loci in the indicated plants by small RNA gel blot. miR168 and U6 were probed as loading controls. The positions of RNA size markers, electrophoresed in parallel, are shown to the left of the blots. The blots were stripped and reprobed multiple times.

(C) Venn diagrams showing the numbers of affected siRNA loci that overlap between *nrpd1-3*, *nrpe1-11*, and each of the *iyo-4*, *qqt2-2*, and *nrpb/d/e11-1* mutants as well as between *iyo-4* and *qqt2-2*.

(D) Detection of Pol V-dependent transcripts produced from representative loci in the indicated plants by RT-PCR. *ACTIN* was amplified as a control. PCR reactions without reverse transcription (no RT) were performed as controls to test for DNA contamination.

(Kolodziej and Young, 1991; Kimura et al., 1997; Hazbun et al., 2003), RPAP1 associates with RPB2 and RPB3 subunits of human Pol II in the cytoplasm before a complete Pol II enzyme is assembled and nuclear imported (Jeronimo et al., 2004; Boulon et al., 2010; Forget et al., 2010). Similar to the case of IYO, QQT2's yeast homolog NPA3 and human homolog GPN1 were reported to mediate Pol II assembly and nuclear import (Forget et al., 2010; Carré and Shiekhattar, 2011; Staresincic et al., 2011; Minaker et al., 2013; Niesser et al., 2015). These previous findings, together with the evidence that Pol IV and Pol V are considered to be specialized forms of Pol II (Ream et al., 2009), led us to propose that IYO and QQT2 regulate the production of Pol IV-dependent

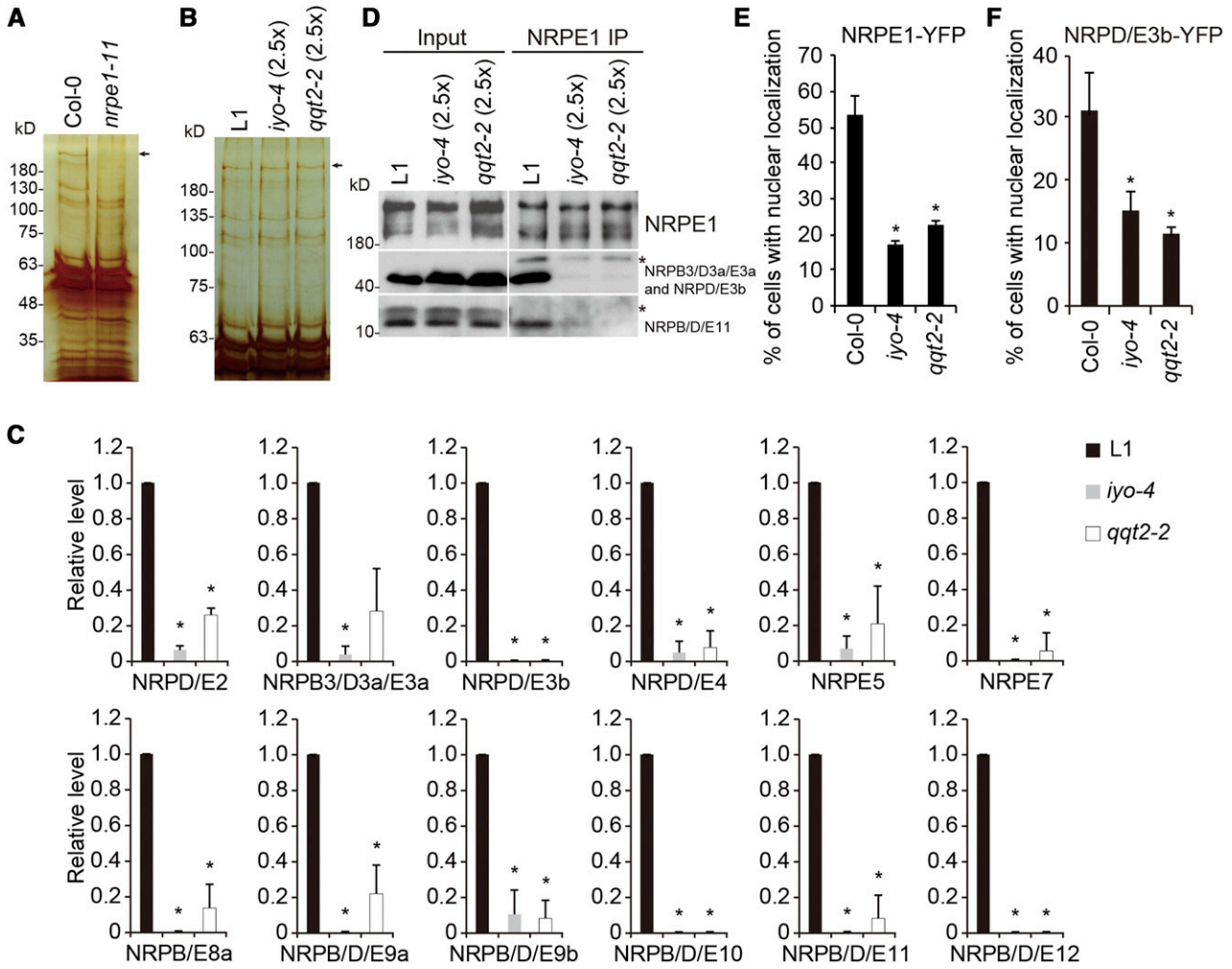

Figure 4. Effects of the *iyo-4* and *qqt2-2* Mutations on Pol V Assembly.

(A) Silver-stained SDS-PAGE gel of the purified Pol V complex. The Pol V complex was immunopurified using an antibody against NRPE1. The position of NRPE1 is indicated.

(B) Silver-stained SDS-PAGE gel of the Pol V complex purified from L1, *iyo-4*, and *qqt2-2*. Note that 2.5 times more protein extracts from *iyo-4* and *qqt2-2* were used for immunopurification. The position of NRPE1 is indicated.

(C) Label-free mass spectrometry-based quantification of NRPE1-associated Pol V subunits in L1, *iyo-4*, and *qqt2-2*. The levels of NRPE1-associated Pol V subunits were normalized against the NRPE1 level. The relative levels of NRPE1-associated subunits in *iyo-4* and *qqt2-2* were determined relative to the levels in L1, which were set at 1. Error bars represent SD from the mean value of three biological replicates. Asterisks indicate a significant difference between L1 and the mutants (Student's *t* test, $P < 0.05$).

(D) Detection of the association between NRPE1 and other Pol V subunits. NRPE1 was immunopurified from L1, *iyo-4*, and *qqt2-2*. Note that 2.5 times more protein extracts from *iyo-4* and *qqt2-2* were used for immunopurification. NRPB3/D3a/E3a (and NRPD/E3b) and NRPB/D/E11 were detected by homemade antibodies. Asterisks indicate nonspecific bands. The positions of molecular mass markers are shown on the left of the blots.

(E) and **(F)** Percentages of protoplast cells with nuclear NRPE1-YFP **(E)** and NRPD/E3b-YFP **(F)** signals in Col-0, *iyo-4*, and *qqt2-2*. Error bars represent SD from the mean value of three biological replicates. Asterisks indicate a significant difference between Col-0 and the mutants (Student's *t* test, $P < 0.05$). At least 250 protoplasts from three independent experiments were counted for each protein to generate the diagram.

Table 1. Identification of Proteins in Immunopurified IYO and QQT2 Complexes by Mass Spectrometry

Protein	AGI Code	Score	Coverage (%)	Unique Peptides	No. of PSMs
IYO-YFP-HA					
IYO	At4g38440	9862.54	88.40	159	3598
NRPD/E2	At3g23780	9.69	7.59	7	8
NRPB3/D3a/E3a	At2g15430	64.72	64.58	20	35
NRPB/D/E10	At1g11475	97.75	35.21	4	57
NRPB/D/E11	At3g52090	14.60	52.59	6	7
NRPB/D/E12	At5g41010	1.87	15.69	1	1
NRPB2	At4g21710	152.54	33.25	42	62
QQT1	At5g22370	4.37	7.05	2	2
QQT2	At4g21800	3.54	9.50	3	3
QQT2-YFP					
QQT2	At4g21800	25563.19	75.46	37	6222
NRPB3/D3a/E3a	At2g15430	109.08	42.95	10	30
NRPB/D/E6a	At5g51940	2.22	4.86	1	1
NRPB/D/E9a	At3g16980	2.88	7.89	1	1
NRPB/D/E10	At1g11475	2.89	12.68	1	1
NRPB/D/E11	At3g52090	31.84	38.79	4	11
NRPB/D/E12	At5g41010	4.56	15.69	1	2
NRPB1	At4g35800	212.46	17.18	32	74
NRPB2	At4g21710	139.76	21.30	25	49
NRPB/D5	At3g22320	37.05	38.05	8	13
RPAP2 homolog	At5g26760	40.97	10.75	9	18
GPN3 homolog	At4g12790	52.77	17.71	5	18

siRNA and Pol V transcripts through regulating Pol IV and Pol V assembly.

We first investigated the role of IYO and QQT2 in Pol V assembly. We immunopurified Pol V holoenzyme using an antibody specifically recognizing a 16-amino acid sequence within NRPE1 (Huang et al., 2009) (Figure 4A) and analyzed proteins associated with NRPE1 by performing mass spectrometry. In line with previous identification of Pol V subunits using recombinant NRPE1 (Ream et al., 2009), we detected 11 Pol V subunits in the NRPE1 immunoprecipitates (Supplemental Table 2 and Supplemental Data Set 1). These included subunits unique to Pol V (NRPE5 and NRPE7), shared by Pol IV and Pol V (NRPD/E2, NRPD/E3b, and NRPD/E4), shared by Pol II and Pol V (NRPB/E8a) or shared by all Pol II, Pol IV, and Pol V (NRPB3/D3a/E3a, NRPB/D/E9a, NRPB/D/E9b, NRPB/D/E11, and NRPB/D/E12) (Ream et al., 2009; Law et al., 2011). The known Pol V-interacting protein RDM4/DMS4 was also detected (He et al., 2009b; Kanno et al., 2010). We then employed label-free quantitative mass spectrometry to determine the relative amounts of different subunits associated with NRPE1, in *iyo-4* and *qqt2-2* (Figure 4B). The levels of all of the other Pol V subunits associated with NRPE1 were either greatly reduced or eliminated in *iyo-4* and *qqt2-2*, suggesting failure of Pol V assembly in these two mutants (Figure 4C; Supplemental Table 3 and Supplemental Data Set 1).

To validate our mass spectrometry results, we conducted coimmunoprecipitation experiments using similar amounts of NRPE1 immunoprecipitates. Consistently, we found that NRPE1 did not associate with other Pol V subunits in *iyo-4* and *qqt2-2* (Figure 4D; Supplemental Figures 3A to 3C). To determine whether unassembled Pol V subunits were retained in the cytoplasm, we transiently expressed *NRPE1-YFP* and *NRPD/E3b-YFP* in protoplasts isolated from Col-0, *iyo-4*, and *qqt2-2* and counted the amount and calculated the percentage of protoplasts with nuclear YFP signal in each background. More than 50% and 30% Col-0 protoplasts had nuclear NRPE1-YFP and NRPD/E3b-YFP signals, respectively. However, the ratio dropped below 25% and 15%, respectively when the protoplasts harbored *iyo-4* and *qqt2-2* backgrounds (Figures 4E and 4F; Supplemental File 1). These results suggest that Pol V, like Pol II, needs to be fully assembled before being imported into the nucleus, but in *iyo-4* and *qqt2-2*, Pol V is unable to be efficiently assembled and imported into the nucleus.

IYO and QQT2 Bind the NRPE3 Subassembly to Form an Assembly Intermediate

According to the current model for Pol II assembly in yeast and humans (Wild and Cramer, 2012), we proposed that the assembly of Pol V holoenzyme could involve the formation and sequential assembly of NRPE3, NRPE2, and NRPE1 subassemblies (Supplemental Figure 4). This led us to ask which step(s) in Pol V assembly involve IYO and QQT2. To address this question, we complemented the *iyo-4* and *qqt2-2* mutants with IYO-YFP-HA and QQT2-YFP, respectively, and analyzed proteins associated with IYO-YFP-HA and QQT2-YFP after immunopurification using mass spectrometry (Supplemental Figures 5A and 5B). Two biological replicates (in which plant growth, immunoprecipitation, and mass spectrometry were performed twice independently) were performed and similar results were obtained. Intriguingly, all four presumable subunits of NRPE3 subassembly, NRPB3/D3a/E3a, NRPB/D/E10, NRPB/D/E11, and NRPB/D/E12, were recovered in both IYO and QQT2 immunoprecipitates (Table 1; Supplemental Data Set 1). Immunoblot analysis also detected NRPB3/D3a/E3a (and/or NRPD/E3b) and NRPB/D/E11 in IYO

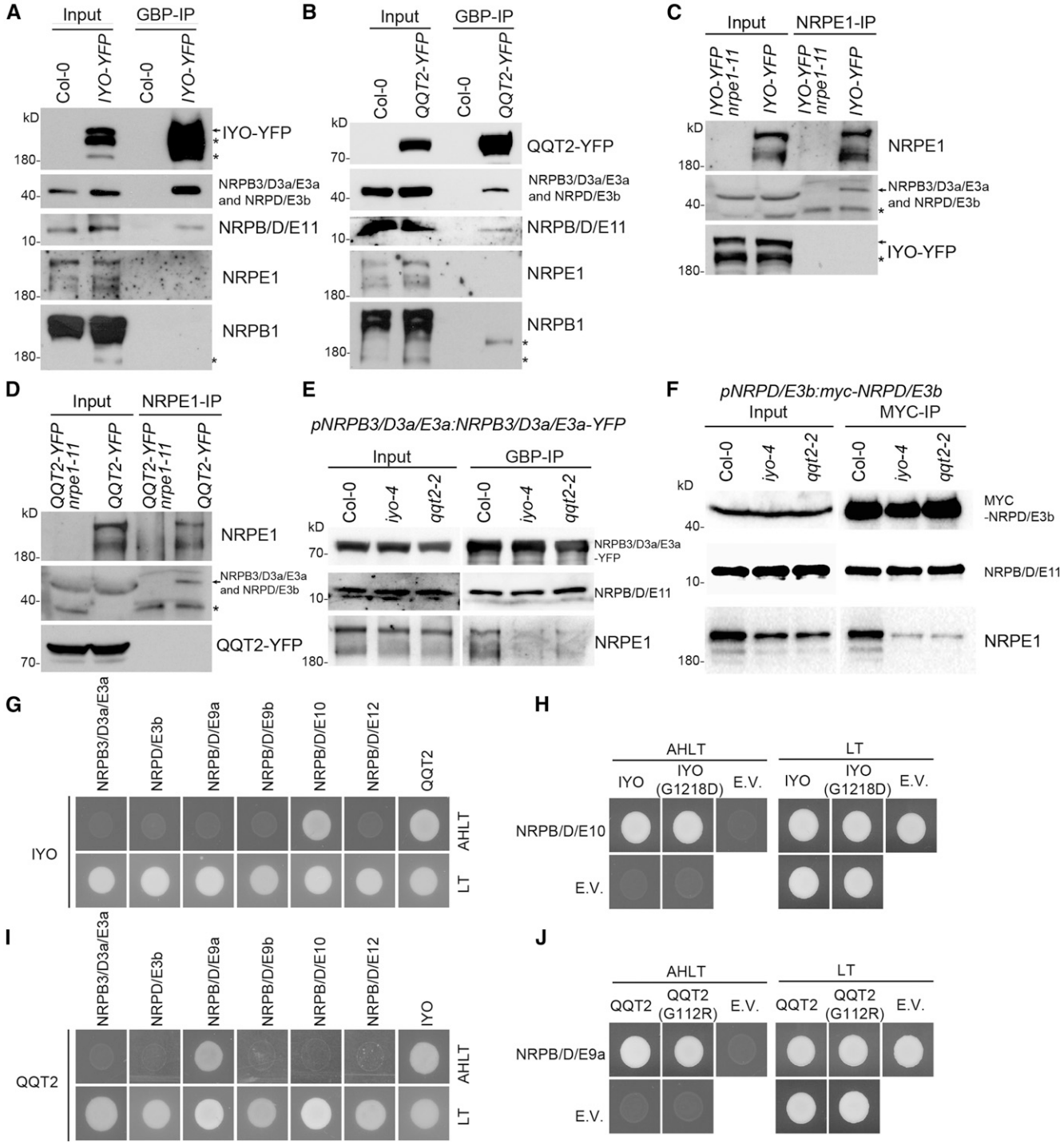

Figure 5. IYO and QQT2 Associate with the NRPE3 Subassembly.

(A) and **(B)** Detection of the association of IYO **(A)** and QQT2 **(B)** with NRPB3/D3a/E3a (and NRPD/E3b), NRPB/D/E11, NRPE1, and NRPB1. IYO-YFP and QQT2-YFP were immunopurified from the transgenic lines expressing IYO-YFP or QQT2-YFP using GBP-conjugated beads. NRPB3/D3a/E3a (and NRPD/E3b), NRPB/D/E11, NRPE1, and NRPB1 were detected in the immunoprecipitates using homemade antibodies. Asterisks indicate non-specific bands. The positions of molecular mass markers are shown on the left of the blots.

(C) and **(D)** Detection of the association of NRPE1 with IYO **(C)** and QQT2 **(D)**. NRPE1 was immunopurified from *IYO-YFP* and *QQT2-YFP* transgenic lines in Col-0 or *nrpe1-11* background using NRPE1 antibody. IYO-YFP and QQT2-YFP were detected in the immunoprecipitates using a GFP antibody, and NRPB3/D3a/E3a (and NRPD/E3b) was detected using a homemade antibody. Asterisks indicate nonspecific bands. The positions of molecular weight markers are shown on the left of the blots.

and QQT2 immunoprecipitates (Figures 5A and 5B). These results showed consistency with previous findings that IYO associates with NRPB3/D3a/E3a, NRPB/D/E10, and NRPB/D/E11 subunits of Pol II in Arabidopsis (Sanmartín et al., 2011; Muñoz et al., 2017).

To further confirm that IYO and QQT2 associate with the NRPE3 subassembly, we generated transgenic plants expressing NRPB3/D3a/E3a-YFP under the control of its native promoter and immunopurified proteins associated with NRPB3/D3a/E3a-YFP (Supplemental Figure 5C). Mass spectrometric analysis detected all subunits comprising Pol II, Pol IV, and Pol V in the NRPB3/D3a/E3a-YFP immunoprecipitates (Supplemental Table 4 and Supplemental Data Set 1). The Pol IV-interacting protein RDR2 (Haag et al., 2012) and the Pol II- and Pol V-interacting protein RDM4/DMS4 (He et al., 2009b; Kanno et al., 2010) were also detected. Importantly, both IYO and QQT2 were pulled down by NRPB3/D3a/E3a-YFP (Supplemental Table 3 and Supplemental Data Set 1).

It was highly interesting to us that IYO and QQT2 could not pull down NRPE1 (Table 1, Figures 5A and 5B; Supplemental Data Set 1), raising the possibility that IYO and QQT2 do not exist within the Pol V holoenzyme. Indeed, IYO and QQT2 were not detected when Pol V holoenzyme was isolated using the NRPE1 antibody (Supplemental Table 2 and Supplemental Data Set 1) and coimmunoprecipitation experiments confirmed that NRPE1 could not pull down IYO and QQT2 (Figures 5C and 5D). These data suggest a model in which IYO and QQT2 associate with the NRPE3 subassembly to form an assembly intermediate and dissociate from Pol V once Pol V assembly is complete.

To examine whether IYO and QQT2 function prior to or after the formation of NRPE3 subassembly, we analyzed the association between NRPE3 subunits and NRPB/D/E11 in the *iyo-4* and *qqt2-2* mutants. The association of NRPB3/D3a/E3a and NRPD/E3b with NRPE1 was disrupted in the *iyo-4* and *qqt2-2* mutants, but their association with NRPB/D/E11 remained intact (Figures 5E and 5F), suggesting that IYO and QQT2 execute their function after the formation of NRPE3 subassembly.

To better understand how IYO and QQT2 function, we probed the direct interaction between IYO or QQT2 with specific Pol V subunits by performing yeast two-hybrid assays. IYO interacted exclusively with NRPB/D/E10, which belongs to the NRPE3 subassembly, while QQT2 interacted exclusively with NRPB/D/E9a, a subunit of NRPE2 subassembly (Figures 5G and 5H). The amino acid changes (G1218D in IYO and G112R in QQT2) introduced by the *iyo-4* mutation and the *qqt2-2* mutation did not disrupt the direct interactions of IYO and QQT2 with specific Pol V subunits (Figures 5I and 5J), suggesting that failure of Pol V assembly in the mutants is not because the association of IYO and QQT2 with Pol V subunits was prevented.

IYO and QQT2 Are Mutually Dependent for Their Association with NRPE3

QQT2 was present in IYO immunoprecipitates (Muñoz et al., 2017) (Table1; Supplemental Data Set 1), suggesting that IYO and QQT2 could interact with each other. Using yeast two-hybrid and bimolecular fluorescence complementation (BiFC) assays, we demonstrated that IYO and QQT2 indeed interact (Figures 6A and 6B). Nuclear and cytoplasmic fractionation revealed that QQT2 is exclusively distributed in the cytoplasm and IYO is present in both the cytoplasm and the nucleus (Supplemental Figures 6A and 6B), suggesting that IYO and QQT2 interact primarily in the cytoplasm. Interestingly, the G1218D amino acid change of IYO and the G112R change of QQT2 abolished the interaction between IYO and QQT2 (Figure 6A), suggesting that the interaction between IYO and QQT2 is important for Pol V assembly. To determine whether IYO and QQT2 cooperatively regulate Pol V assembly, we examined their association with NRPB3/D3a/E3a in different mutants. The *qqt2-2* mutation severely disrupted the association of IYO with NRPB3/D3a/E3a (and/or NRPD/E3b) (Figure 6C). Similarly, the *iyo-4* mutation severely disrupted the association of QQT2 with NRPB3/D3a/E3a (and/or NRPD/E3b) (Figure 6D). These results suggest that IYO and QQT2 are mutually dependent for their association with NRPE3 subassembly.

IYO and QQT2 Are Also Required for Pol II and Pol IV Assembly

We finally investigated whether IYO and QQT2 are also required for the assembly of Pol II and Pol IV. We examined the association between NRPB1 and other Pol II subunits in *iyo-4* and *qqt2-2* by label-free mass spectrometry. We found that the association of all of the other Pol II subunits with NRPB1 remained unaltered in the *iyo-4* and *qqt2-2* mutants (Figure 7A; Supplemental Figure 7A, Supplemental Table 5, and Supplemental Data Set 1). Coimmunoprecipitation experiment confirmed intact association between NRPB1 and NRPB3 in these two mutants (Supplemental Figure 7B). However, the association of some other Pol II subunits with NRPB1 was reduced in amiR-IYO (Figure 7A; Supplemental Figure 7A, Supplemental Table 5, and Supplemental Data Set 1). These results suggest that *iyo-4* and *qqt2-2* are unique mutations that do not affect Pol II assembly, but IYO and QQT2 are most likely required for Pol II assembly.

We attempted to examine Pol IV assembly in *iyo-4* and *qqt2-2* by detecting the association between NRPD1-Flag with other Pol IV subunits. However, the attempts were unsuccessful because, even from the *NRPD1-Flag* transgenic plants in Col-0 background, immunopurification of NRPD1-Flag yielded few other subunits of RNA polymerases. We then examined Pol IV assembly in *iyo-4* and *qqt2-2* indirectly. We immunopurified NRPD/E3b-YFP, a subunit shared by Pol IV and Pol V (Law et al., 2011), from Col-0, *iyo-4*, and *qqt2-2* (Supplemental Figure 7C) and compared the amounts of NRPD1 and other subunits associated with NRPD/E3b-YFP between Col-0 and the mutants. Except NRPB3/D3a/E3a and NRPB/D/E11, the amounts of NRPD/E3b-YFP-associated NRPD1 and other subunits were either greatly reduced or eliminated in *iyo-4* and *qqt2-2* (Figure 7B; Supplemental Table 6 and Supplemental Data Set 1), suggesting failure of Pol IV assembly in these two mutants. Thus, IYO and QQT2 are also required for Pol IV assembly.

DISCUSSION

Plants have evolved two RNA polymerases, Pol IV and Pol V, specialized for RdDM. How these RNA polymerases are

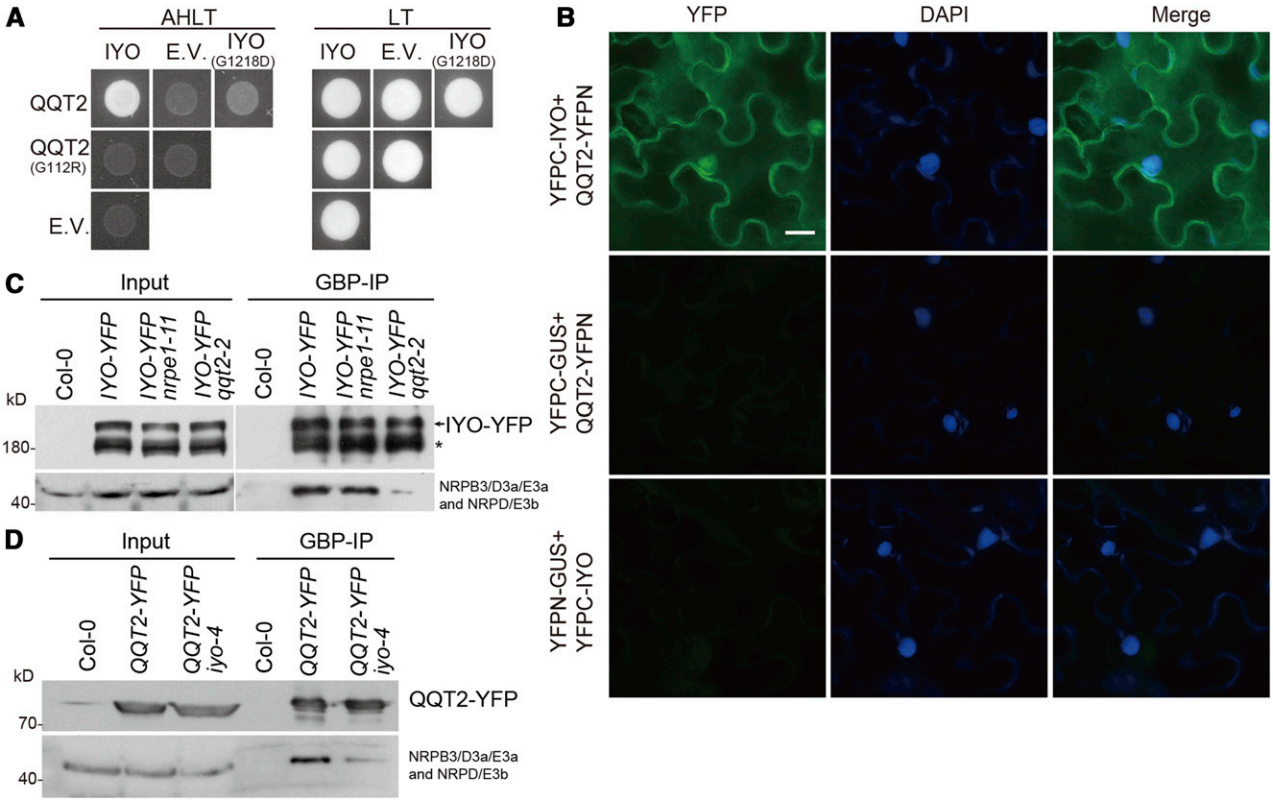

Figure 6. IYO and QQT2 Interact and Depend on Each Other to Associate with NRPE3.

(A) Detection of the interaction between IYO and QQT2 by yeast two-hybrid analysis. Yeast cells expressing the indicated proteins from the pGAD-T7 (AD) and pGBK-T7 (BD) vectors were grown on medium lacking Leu and Trp (-LT) or medium lacking Ade, His, Leu, and Trp (-AHLT). E.V., empty vector.
(B) Detection of the interaction between IYO and QQT2 by BiFC. *Nicotiana benthamiana* leaves were infiltrated with the indicated constructs and examined by fluorescence microscopy. Bar = 20 μm.
(C) Detection of the association of IYO with NRPB3/D3a/E3a (and NRPD/E3b) in Col-0, *nrpe1-11*, and *qqt2-2*. IYO-YFP was immunopurified from the transgenic lines expressing IYO-YFP in Col-0, *nrpe1-11*, and *qqt2-2* backgrounds using GBP-conjugated beads. NRPB3/D3a/E3a (and NRPD/E3b) was detected in the immunoprecipitates using a homemade antibody. The asterisk indicates nonspecific bands.
(D) Detection of the association of QQT2 with NRPB3/D3a/E3a (and NRPD/E3b) in Col-0, *nrpe1-11*, and *iyo-4*. QQT2-YFP was immunopurified from the transgenic lines expressing IYO-YFP in Col-0, *nrpe1-11*, and *iyo-4* backgrounds using GBP-conjugated beads. NRPB3/D3a/E3a (and NRPD/E3b) was detected in the immunoprecipitates using a homemade antibody.

assembled remains elusive. In this study, the isolation of the viable *iyo-4* and *qqt2-2* mutants (Figure 1) that are defective in RdDM (Figure 2) and in producing both Pol IV-dependent siRNA and Pol V-dependent transcripts (Figure 3) provided us a unique opportunity to dissect the role of IYO and QQT2 in the assembly of RNA polymerases. We found that Pol V failed to be assembled

Figure 5. (continued).

(E) and **(F)** Detection of the association of NRPB3/D3a/E3a **(E)** and NRPD/E3b **(F)** with NRPB/D/E11 in Col-0, *iyo-4*, and *qqt2-2*. NRPB3/D3a/E3a-YFP and myc-NRPD/E3b were immunopurified from the transgenic lines expressing NRPB3/D3a/E3a-YFP and myc-NRPD/E3b in Col-0, *iyo-4*, and *qqt2-2* backgrounds using GBP-conjugated beads and MYC beads, respectively. NRPB/D/E11 and NRPE1 were detected in the immunoprecipitates using homemade antibodies. The positions of molecular mass markers are shown on the left of the blots.
(G) and **(H)** Detection of the interactions of IYO **(G)** and QQT2 **(H)** with indicated Pol V subunits by yeast two-hybrid analysis. Yeast cells expressing the indicated proteins from the pGAD-T7 (AD) and pGBK-T7 (BD) vectors were grown on medium lacking Leu and Trp (-LT) or medium lacking Ade, His, Leu, and Trp (-AHLT). E.V., empty vector.
(I) and **(J)** Detection of the interactions of mutant forms of IYO **(I)** and QQT2 **(J)** with NRPB/D/E10 and NRPB/D/E9a, respectively, by yeast two-hybrid analysis. Yeast cells expressing the indicated proteins from the pGAD-T7 (AD) and pGBK-T7 (BD) vectors were grown on medium lacking Leu and Trp (-LT) or medium lacking Ade, His, Leu, and Trp (-AHLT).

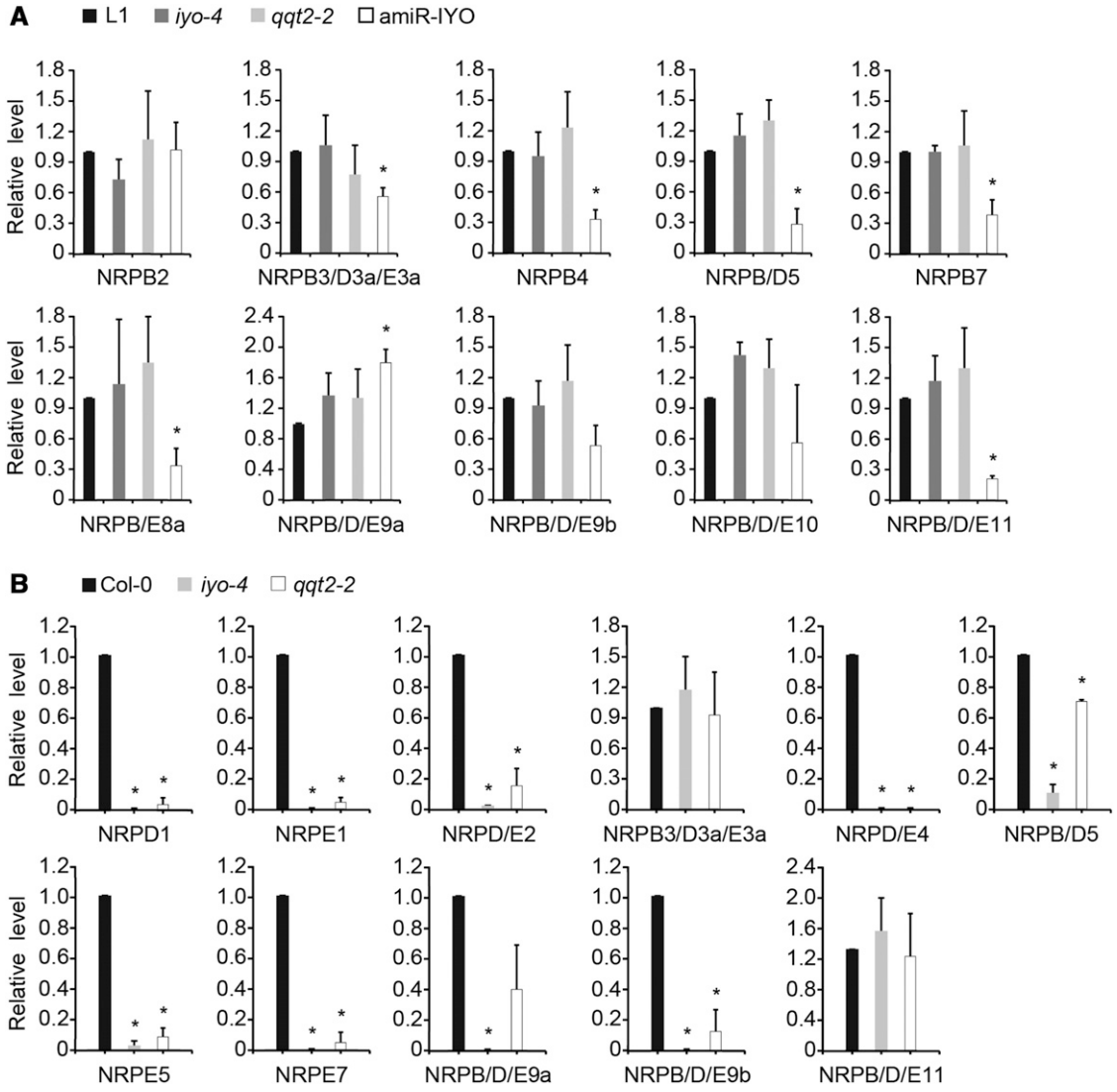

Figure 7. Effects of the *iyo-4* and *qqt2-2* Mutations on the Assembly of Pol II and Pol IV.

(A) Label-free mass spectrometry-based quantification of NRPB1-associated Pol II subunits in L1, *iyo-4*, *qqt2-2*, and amiR-IYO. The levels of NRPB1-associated Pol II subunits were normalized against the NRPB1 level. The relative levels of NRPB1-associated subunits in *iyo-4* and *qqt2-2* were determined relative to the levels in Col-0, which were set at 1. Error bars represent SD from the mean value of three biological replicates. Asterisks indicate a significant difference between L1 and amiR-IYO (Student's *t* test, $P < 0.05$).

(B) Label-free mass spectrometry-based quantification of NRPD/E3b-YFP-associated Pol IV/V subunits in Col-0, *iyo-4*, and *qqt2-2*. The levels of NRPD/E3b-YFP-associated Pol IV/V subunits were normalized against the NRPD/E3b-YFP level. The relative levels of NRPD/E3b-YFP-associated subunits in *iyo-4* and *qqt2-2* were determined relative to the levels in Col-0, which were set at 1. Error bars represent SD from the mean value of three biological replicates. Asterisks indicate a significant difference between Col-0 and the mutants (Student's *t* test, $P < 0.05$).

in the *iyo-4* and *qqt2-2* mutants (Figure 4), suggesting that IYO and QQT2 are required for Pol V assembly. We then tried to identify at which step they function and found that they associated with NRPE3 subassembly (Table 1, Figures 5A and 5B; Supplemental Table 3). The *iyo-4* and *qqt2-2* mutations did not affect the association of NRPB3/D3a/E3a (and/or NRPD/E3b) with NRPB/D/E11 but compromised their association with NRPE1 (Figures 5E and 5F), suggesting that they function after the formation of NRPE3 subassembly. NRPD/E2 and NRPB2 peptides were detected in the IYO and QQT2 immunoprecipitates (Table 1), and IYO interacted with NRPB/D/E10, a subunit of the NRPE3 subassembly, while QQT2 interacted with NRPB/D/E9a, a subunit of NRPE2 subassembly (Figures 5G and 5H), suggesting that IYO and QQT2 may play a role in bridging the NRPE3 and NRPE2 subassemblies. The *qqt2-2* mutation impaired the association of IYO with NRPB3/D3a/E3a (and/or NRPD/E3b) (Figure 6C), suggesting that the bridging between the NRPE3 and NRPE2 subassemblies could stabilize

the NRPE3 subassembly. Interestingly, both IYO and QQT2 failed to pull down NRPE1 and vice versa (Table 1, Figures 5A to 5D; Supplemental Table 2), implying that they are released from Pol V holoenzyme once Pol V assembly is complete. We further found that IYO and QQT2 interacted and were mutually dependent for their association with NRPB3/D3a/E3a (and NRPD/E3b) (Table 1, Figure 6). Based on these observations, we propose a model for the assembly of Pol V in Arabidopsis (Figure 8). Like the assembly of Pol II in yeast and humans (Wild and Cramer, 2012), the assembly of Pol V starts with the dimerization of NRPE3 and NRPE11 and the formation of the NRPE3 subassembly. IYO and QQT2 then jointly associate with the NRPE3 subassembly and facilitate the assembly of Pol V. IYO and QQT2 dissociate once the Pol V holoenzyme is fully assembled.

Pol II assembly was not affected by *iyo-4* and *qqt2-2*. However, Pol II assembly was greatly affected in amiR-IYO (Figure 7A). These results, together with the results that IYO and QQT2 coimmunoprecipitated with Pol II-specific subunits (Table 1) and the observation that the level of NRPB1 was decreased in a strong *IYO* allele *iyo-1* (Sanmartín et al., 2011), suggest that IYO and QQT2 are also required for Pol II assembly. We further found that IYO and QQT2 are required for Pol IV assembly (Figure 7B). Because Pol II, Pol IV, and Pol V have highly similar subunit compositions (Ream et al., 2009; Tucker et al., 2010; Wang and Ma, 2015), we propose that the model for Pol V should also be applied to Pol II and Pol IV (Supplemental Figure 8).

In addition to QQT2, IYO also coimmunoprecipitated with QQT1 (homolog of human GPN2) (Table 1). QQT2 coimmunoprecipitated with GPN3 homolog (Table 1) and was previously reported to interact with QQT1 (Lahmy et al., 2007). Since human GPN1, GPN2, and GPN3 are all implicated in Pol II assembly (Boulon et al., 2010; Forget et al., 2010; Wild and Cramer, 2012; Niesser et al., 2015), we propose that the assembly of Pol II, Pol IV, and Pol V in Arabidopsis also requires QQT1 and the GPN3 homolog. In our study, the effects of *qqt2-2* on RdDM were not as profound as those caused by *iyo-4*, *nrpb/d/e11-1*, *nrpd1-3*, and *nrpe1-11* (Figure 2). Compared with *iyo-4*, the effects of *qqt2-2* on Pol IV and Pol V assembly were slightly weaker. The functional redundancy of QQT1, QQT2, and the GPN3 homolog could account for such moderate effects of *qqt2-2*, although they could also be attributable to *qqt2-2* being a weak allele.

Studies in yeast revealed that QQT2's homolog NPA3 serves as an assembly chaperone that interacts with the hydrophobic peptides of Pol II subunits. Upon interaction, NPA3 changes its conformation to bind GTP and opens a pocket that accommodates a Pol II subunit. When GTP is hydrolyzed, the NPA3-trapped Pol II subunit is released to associate with other assembled Pol II subunits (Niesser et al., 2015). QQT2 likely adopts similar mechanisms for Pol V assembly. However, whether QQT2 has GTPase activity requires further investigation. In addition to being involved in Pol II assembly, NPA3 and human GPN1 shuttle between the cytoplasm and the nucleus to mediate nuclear targeting of fully assembled Pol II (Forget et al., 2010; Carré and Shiekhattar, 2011; Staresincic et al., 2011). However, our results revealed that QQT2 is exclusively distributed in the cytoplasm (Supplemental Figure 6), suggesting that QQT2 may not be able to shuttle in and out of the nucleus.

In summary, we report that IYO and QQT2 are assembly factors common to Pol II, Pol IV, and Pol V. Since the yeast and human homologs of IYO and QQT2 were all suggested to be involved in Pol II assembly (Jeronimo et al., 2004; Boulon et al., 2010; Forget et al., 2010; Carré and Shiekhattar, 2011; Minaker et al., 2013; Niesser et al., 2015), the role of IYO and QQT2 in polymerase assembly appears to be highly conserved in eukaryotes.

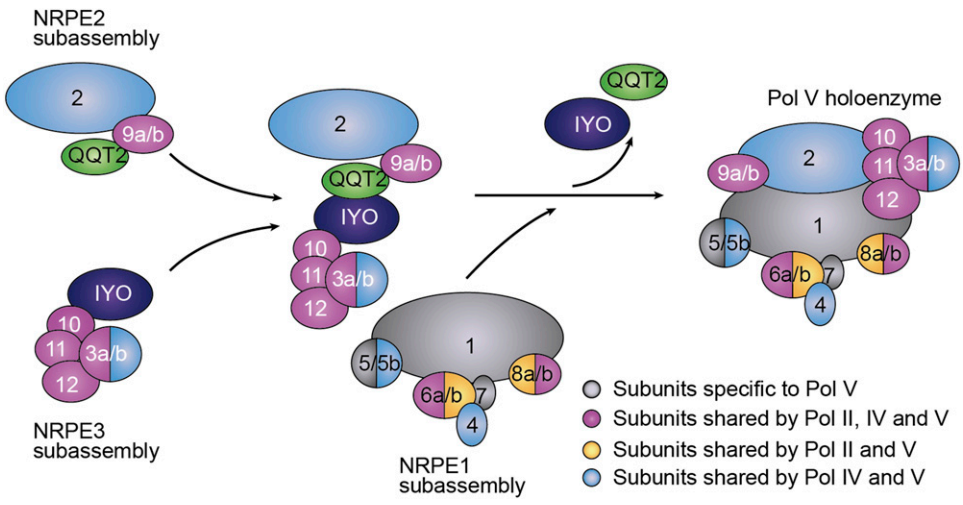

Figure 8. A Model for the Role of IYO and QQT2 in Pol V Assembly.

The assembly of Pol V involves the formation of NRPE3, NRPE2, and NRPE1 subassemblies. IYO associates with the NRPE3 subassembly and QQT2 associates with the NRPE2 subassembly and jointly facilitate the assembly of Pol V holoenzyme. IYO and QQT2 are released once the Pol V holoenzyme is fully assembled.

METHODS

Plant Materials and Growth Conditions

The *Arabidopsis thaliana* transgenic line (Col-0 ecotype) expressing GFP-AGO4 under the control of native *AGO4* promoter, designated here as L1, was generated previously (Ye et al., 2012). The *nrpd1-3* (SALK_128428) and *nrpe1-11* (SALK_029919) mutants were described previously (Onodera et al., 2005; Pontes et al., 2006). The *NRPD1-Flag* transgenic line was previously described (He et al., 2009a).

All seeds were surface-sterilized with 0.5% sodium hypochlorite (NaClO) before being sown on half-strength Murashige and Skoog plates. After vernalization at 4°C for at least 24 h, the plates were placed in a growth chamber. Twelve-day-old seedlings were transferred to soil or frozen in liquid nitrogen immediately and stored at −80°C until use. All plants were grown under long-day conditions (16 h light, 22°C/8 h dark, 18°C). Growth light was provided by color 865 fluorescent tubes (Philips; TLD, 36 W).

Mutagenesis and Screening

L1 was used as the parental line for mutagenesis. About 3400 L1 seeds were treated with 0.4% ethyl methanesulfonate in 100 mM KPO4 buffer (pH 7.5) for 8 h at room temperature with gentle agitation. They were subsequently washed 20 times with sterilized water and sown on half-strength Murashige and Skoog plates containing hygromycin B (25 μg/mL) before being transferred to soil. Seeds from two plants were mixed as a pool. Approximately 40 seeds from each pool were grown vertically on plates containing hygromycin B. GFP-AGO4 expression in the hypocotyl region of seedlings was observed under a stereomicroscope with an epifluorescence illuminator (Nikon SMZ1500). The mutants with reduced GFP signal were selected for Chop-PCR analysis of their DNA methylation levels at selected RdDM loci. The mutants with DNA hypomethylation were maintained by backcrossing to the L1 plants and kept for molecular mapping.

Cloning of *DAS1*, *DAS2*, and *DAS3*

To map *das1*, *das2*, and *das3*, the mutants (Col-0 ecotype) were crossed with the wild-type plants in Landsberg *erecta* ecotype. In the F2 generation, more than 35 plants with reduced GFP-AGO4 fluorescence signal and DNA hypomethylation were selected and pooled. The genomes of the pools were sequenced and analyzed as previously described (Fang et al., 2015).

Plasmid Construction

For complementation of the *das* mutants, full-length genomic DNA of *IYOQQT2* and *NRPB/D/E11* were amplified and cloned into pENTR/D-TOPO (Invitrogen) and subsequently recombined into the binary destination vector pEarleyGate302 (Earley et al., 2006), creating *IYO-Flag*, *QQT2-Flag*, and *NRPB/D/E11-Flag* constructs. The coding sequences of *IYO*, *QQT2*, and genes encoding Pol subunits were either cloned into pCambia1300-(35S)-N1-YFP (Fang and Spector, 2007) or pEarleyGate101 and pEarleyGate203 vectors (Earley et al., 2006), creating *IYO-YFP-HA*, *QQT2-YFP*, *NRPB3/D3a/E3a-YFP*, *NRPD/E3b-YFP*, *myc-NRPD/E3b*, *myc-NRPB/E8a*, *myc-NRPB/D/E9a*, and *myc-NRPB/D/E9b* constructs. These constructs were then transformed into Col-0, *iyo-4*, or *qqt2-2* plants. The constructs for yeast two-hybrid and BiFC experiments were obtained by cloning of each coding sequence into pGADT7 and pGBKT7, and pCambia1300-35S-N1-YFPN and pCambia1300-35S-N1-YFPC (Fang and Spector, 2007), respectively. The constructs expressing amiR-IYO or amiR-QQT2 were made as described (Schwab et al., 2006). Primers used for generating constructs are listed in Supplemental Table 7.

Generation of Antibodies

A synthetic peptide NRPE1BD (CDKKNSETESDAAAWG) (Huang et al., 2009) was used to raise rabbit polyclonal antibody against NRPE1. Full-length *NRPB3/D3a/E3a* and *NRPB/D/E11* cDNAs were amplified and cloned into pET28a to generate the constructs expressing His-NRPB3/D3a/E3a and His-NRPB/D/E11, respectively. The constructs were transformed into *Escherichia coli* (BL21) cells. The cells were lysed with a buffer containing 20 mM Tris-HCl (pH8.0) and 8 M urea. His-NRPB3/D3a/E3a and His-NRPB/D/E11 were purified on HisTrap HP columns (GE 29051021) and used to raise rabbit polyclonal antibodies against NRPB3/D3a/E3a (and NRPD/E3b) and NRPB/D/E11.

Immunoprecipitation and Immunoblotting

Ten-day-old seedlings ground in liquid nitrogen were homogenized with extraction buffer (50 mM Tris, pH 7.5, 150 mM NaCl, 5 mM $MgCl_2$, 10% glycerol, 0.2% Nonidet P-40, 5 mM DTT, and 1 tablet/50mL protease inhibitor cocktail). After centrifugation, the supernatant was incubated at 4°C with either Protein A beads/NRPE1 antibody, Protein G beads/NRPB1 antibody, GFP binding protein (GBP)-conjugated beads, or anti-HA affinity gel (Sigma-Aldrich; E6779) for 2 h. The beads were washed with extraction buffer five times for 5 min each time. The NRPE1- and HA-bound protein complexes were then eluted with corresponding peptide solution (0.5 mg/mL) at 16°C for 30 min. The NRPB1- and GBP-bound protein complexes were boiled in SDS loading buffer. The protein samples were then subject to mass spectrometry or immunoblot analysis.

For immunoblot analysis, protein extracts or immunoprecipitates were mixed with SDS loading buffer and boiled for 10 min. Proteins were separated by SDS-PAGE gels, transferred to PVDF membranes, and detected by NRPE1 (1:1000 dilution), NRPB3/D3a/E3a (and/or NRPD/E3b) (1:1000 dilution), NRPB/D/E11 (1:1000 dilution), NRPB1 (Abcam, ab817) (1:2000 dilution), AGO4 (Agrisera, AS09617) (1:1000 dilution), TUBULIN (Sigma-Aldrich) (1:3000 dilution), myc (Roche) (1:3000 dilution), Flag (Sigma-Aldrich) (1:3000 dilution), and GFP (Roche) (1:3000 dilution) antibodies. Goat anti-rabbit IgG-HRP (1:5000 dilution) and goat anti-mouse IgG-HRP (1:5000 dilution) were used as secondary antibodies. The blots were visualized by chemiluminescence.

Locus-Specific Bisulfite Sequencing and Chop-PCR

Genomic DNA was isolated using a DNeasy Plant kit (Qiagen) according to the manufacturer's instructions. Five hundred nanograms of DNA was used for bisulfite sequencing analysis as previously described (Wu et al., 2010). For Chop-PCR, 500 ng of DNA was digested with 10 units of *Hae*III, and PCRs were performed as described (Zhang et al., 2014). Primers are listed in Supplemental Table 7.

Whole-Genome Bisulfite Sequencing and Data Analysis

Libraries for bisulfite sequencing were constructed as previously described (Ye et al., 2016). The libraries were paired-end sequenced on an Illumina HiSeq 2000 platform. For data analysis, low-quality bases were trimmed and clean reads were mapped to the Arabidopsis genome (TAIR10) by BRAT-BW (Harris et al., 2012), allowing three mismatches. Copy duplicates were removed and uniquely mapped reads were retained. The methylation status of each cytosine was calculated by acgt-count (Harris et al., 2012).

CHH hypo-DMRs (differentially methylated regions) were defined as previously described (Law et al., 2013; Ye et al., 2016). Briefly, DNA methylation levels in every 200-bp sliding windows with a step size of 50 bp were compared between the wild type and the mutants. Windows with absolute methylation difference ≥0.1 and Benjamini-Hochberg-adjusted false discovery rate < 0.001 (Fisher's exact test) were defined as DMRs. DMRs in close vicinity (<100 bp) were merged. The bisulfite sequencing

data sets of *drm1/2* and its corresponding wild type were obtained from GSE39901, and CHH hypo-DMRs in *drm1/2* were annotated as RdDM loci.

Small RNA Sequencing and Analysis

Small RNAs of 18 to 30 nucleotides were gel-purified and subjected to library construction as previously described (Mi et al., 2008). The library was sequenced on an Illumina HiSeq 2000 platform and sequencing reads were analyzed as described (Ye et al., 2016). Briefly, the 3′ adapter of sequenced reads were trimmed by cutadapt 1.12 and only reads with the size of 18 to 30 nucleotides were retained. Clean small RNA reads were then mapped to the Arabidopsis genome (TAIR10) with bowtie allowing no mismatches (Langmead et al., 2009). Read counts were normalized to reads per million (RPMs) by the number of clean reads mapped to the genome in each library.

For Venn diagram analysis of siRNA loci that overlap between different mutants, the abundance of siRNAs was summarized in 200-nucleotide nonoverlapping windows and scaled to RPM. The windows that had an abundance of at least 5 RPMs were considered as siRNA-producing loci. When a locus had at least 3-fold reduction in siRNA abundance in *nrpd1-3* in comparison to the wild type, the locus was defined as Pol IV-dependent locus. The same criteria were used for the identification of loci dependent on Pol V, IYO, QQT2, or NRPB/D/E11.

Small RNA Gel Blotting

Gel blot analysis of small RNAs was performed as described (Qi et al., 2005). Briefly, small RNAs were separated by 15% denaturing gel and transferred onto Hybond-N^+ membranes (Amersham). Membranes were UV cross-linked and hybridized to ^{32}P end-labeled oligonucleotide probes. The sequences of the probes are listed in Supplemental Table 7.

RNA Analyses

Total RNA was extracted with the Trizol reagent (Invitrogen) from 10-d-old seedlings, treated with DNase I (Promega) to remove DNA contamination, and reverse-transcribed by M-MLV (Invitrogen) using oligo(dT) primers. Quantitative RT-PCR was performed with SYBR Premix Ex Taq (Takara). *TUBULIN* mRNA was detected in parallel and used for data normalization. The detection of Pol V-dependent transcripts was performed as previously described (Wierzbicki et al., 2008). Briefly, 1 μg of RNA digested with DNase I (Promega) was reversely transcribed with SuperScript III reverse transcriptase (Invitrogen), 0.5 μL Platinum Taq (Invitrogen), and a gene-specific primer. After heat inactivation of reverse transcriptase, the second primer was added and PCR was performed. For quantitative RT-PCR, the average levels of transcripts from three biological replicates were presented. The same mutant lines and transgenic lines were used. Plant growth and RNA purification were performed three times independently. Primers used for PCR are listed in Supplemental Table 7.

Mass Spectrometry-Based Label-Free Quantification

Total protein extracts were subjected to immunoprecipitation with NRPE1 or NRPB1 antibody. Proteins copurified with NRPE1, NRPB1, or NRPD/E3b-YFP were eluted and subjected to mass spectrometry analysis using nano-LC-MS/MS with an LTQ-Orbitrap XL mass spectrometer. Data were searched using Mascot server and analyzed using the MFPaQ software. The relative amounts of each subunit copurified with NRPE1 or NRPB1 were determined by label-free quantification as described (Silva et al., 2006). Briefly, the mean of the three highest peptides areas was calculated for each subunit. The values of each subunit were then divided by that of NRPE1, NRPB1, or NRPD/E3b-YFP. The relative levels of each subunit were determined relative to the value of the wild type, which was set at 1. The average amounts of each subunit are presented from three biological replicates in which plant growth, immunoprecipitation and label-free mass spectrometry performed three times independently with the same mutant and transgenic lines.

Protoplast Transformation

Protoplast isolation and transfection were performed essentially as described (Yoo et al., 2007). Briefly, protoplasts were isolated from Arabidopsis leaves and incubated with NRPE1-YFP or NRPD/E3b-YFP plasmids in PEG/Ca solution (40% PEG4000 [Fluka], 100 mM $CaCl_2$, and 0.2 M mannitol) for 20 min. After being washed three times with W5 solution (154 mM NaCl, 125 mM $CaCl_2$, 5 mM KCl, 5 mM glucose, and 2 mM MES, pH 5.6), the transformed protoplasts were cultured for 16 h under naturally occurring light. The average percentages of protoplasts with nuclear signal are from three biological replicates in which protoplast isolation and transformation were performed three times independently with the same mutant lines.

Yeast Two-Hybrid Assay

The yeast two-hybrid assay was performed according to the manufacturer's instructions (Clontech). Briefly, pairs of plasmids were cotransformed into the yeast strain AH109. Transformants were first grown on SD/-Leu/-Trp medium and subsequently plated on SD/-Ade/-His/-Leu/-Trp medium.

Agroinfiltration and BiFC Assay

Agroinfiltration and BiFC experiments were performed as described (Fang and Spector, 2007) except that *Nicotiana benthamiana* plants were used. Constructs expressing GUS-fused YFPN or YFPC were used as negative controls.

Fluorescence Microscopy

Images of the agroinfiltrated *N. benthamiana* cells and protoplast cells were acquired with Axio Imager Z2 Upright Microscope equipped with a CCD camera (AxioCam MRm).

Nuclear-Cytoplasmic Fractionation

The nuclear-cytoplasmic fractionation was performed essentially as described (Wang et al., 2011) except that14-d-old seedlings were used.

Accession Numbers

Sequence data from this article can be found in the Arabidopsis Genome Initiative database or the GenBank data library under the following accession numbers: *IYO* (At4g38440), *QQT2* (At4g21800), *AGO4* (At2g27040), *NRPE1* (At2g40030), *NRPD/E2* (At3g23780), *NRPB3/D3a/E3a* (At2g15430), *NRPD/E3b* (At2g15400), *NRPD/E4* (At4g15950), *NRPE5* (At3g57080), *NRPE7* (At4g14660), *NRPB/E8a* (At1g54250), *NRPB/D/E8b* (At3g59600), *NRPB/D/E9a* (At3g16980), *NRPB/D/E9b* (At4g16265), *NRPB/D/E10* (At1g11475), *NRPB/D/E11* (At3g52090), *NRPB/D/E12* (At5g41010), and *NRPD1* (At1g63020). Small RNA deep sequencing and whole-genome bisulfite sequencing data sets generated in this study are deposited in the National Center for Biotechnology Information Gene Expression Omnibus (http://www.ncbi.nlm.nih.gov/geo/) under accession number GSE103326.

Supplemental Data

Supplemental Figure 1. Effects of *nrpd1* and *nrpe1* Mutations on the GFP-AGO4 Protein Level.

Supplemental Figure 2. Characterization of Artificial miRNA Lines of *IYO* and *QQT2.*

Supplemental Figure 3. Effects of the *iyo-4* and *qqt2-2* Mutations on Pol V Assembly.

Supplemental Figure 4. A Model for the Assembly of Pol V.

Supplemental Figure 5. Analyses of Protein Complexes Copurified with IYO, QQT2, or NRPB3/D3a/E3a.

Supplemental Figure 6. Analyses of the Nuclear-Cytoplasmic Distribution of IYO and QQY2.

Supplemental Figure 7. Effects of the *iyo-4* and *qqt2-2* Mutations and *IYO* Knockdown on Pol II and Pol IV Assembly.

Supplemental Figure 8. Models for the Role of IYO and QQT2 in Pol II and Pol IV Assembly.

Supplemental Table 1. Summary of Mutants Isolated in the RdDM Pathway.

Supplemental Table 2. Identification of Proteins in Immunopurified NRPE1 Complex by Mass Spectrometry.

Supplemental Table 3. Label-Free Mass Spectrometric Analysis of NRPE1-Associated Subunits.

Supplemental Table 4. Identification of Proteins in Immunopurified NRPB3/D3a/E3a-YFP Complex by Mass Spectrometry.

Supplemental Table 5. Label-Free Mass Spectrometric Analysis of NRPB1-Associated Subunits.

Supplemental Table 6. Label-Free Mass Spectrometric Analysis of NRPD/E3b-Associated Subunits.

Supplemental Table 7. Oligonucleotides Used in This Study.

Supplemental Data Set 1. Raw Mass Spectrometry Data.

Supplemental File 1. Results of Statistical Analyses.

ACKNOWLEDGMENTS

We thank Yan Li for editing the manuscript. This work was supported by grants from National Natural Science Foundation of China (Grants 31620103908 and 31788103) and National Key Research and Development Program of China (Grant 2016YFA0500800) to Y.Q. Y.Q. is a visiting Investigator of the CAS Center for Excellence in Molecular Plant Sciences.

AUTHOR CONTRIBUTIONS

Y.Q. conceived this project. Y.L., Y.Y., X.F., and Y.Q. designed experiments. Y.L., Y.Y., X.F., X.L., and G.Z. performed the experiments. Y.L., Y.Y., X.F., B.L., and Y.Q. analyzed the data. X.F. and Y.Q. wrote the manuscript.

Received May 17, 2017; revised January 9, 2018; accepted January 17, 2018; published January 18, 2018.

REFERENCES

Boulon, S., Pradet-Balade, B., Verheggen, C., Molle, D., Boireau, S., Georgieva, M., Azzag, K., Robert, M.C., Ahmad, Y., Neel, H., Lamond, A.I., and Bertrand, E. (2010). HSP90 and its R2TP/Prefoldin-like cochaperone are involved in the cytoplasmic assembly of RNA polymerase II. Mol. Cell **39:** 912–924.

Carré, C., and Shiekhattar, R. (2011). Human GTPases associate with RNA polymerase II to mediate its nuclear import. Mol. Cell. Biol. **31:** 3953–3962.

Czeko, E., Seizl, M., Augsberger, C., Mielke, T., and Cramer, P. (2011). Iwr1 directs RNA polymerase II nuclear import. Mol. Cell **42:** 261–266.

Earley, K.W., Haag, J.R., Pontes, O., Opper, K., Juehne, T., Song, K., and Pikaard, C.S. (2006). Gateway-compatible vectors for plant functional genomics and proteomics. Plant J. **45:** 616–629.

Fang, X., Cui, Y., Li, Y., and Qi, Y. (2015). Transcription and processing of primary microRNAs are coupled by Elongator complex in Arabidopsis. Nat. Plants **1:** 15075.

Fang, Y., and Spector, D.L. (2007). Identification of nuclear dicing bodies containing proteins for microRNA biogenesis in living Arabidopsis plants. Curr. Biol. **17:** 818–823.

Forget, D., Lacombe, A.A., Cloutier, P., Al-Khoury, R., Bouchard, A., Lavallée-Adam, M., Faubert, D., Jeronimo, C., Blanchette, M., and Coulombe, B. (2010). The protein interaction network of the human transcription machinery reveals a role for the conserved GTPase RPAP4/GPN1 and microtubule assembly in nuclear import and biogenesis of RNA polymerase II. Mol. Cell. Proteomics **9:** 2827–2839.

Haag, J.R., Ream, T.S., Marasco, M., Nicora, C.D., Norbeck, A.D., Pasa-Tolic, L., and Pikaard, C.S. (2012). In vitro transcription activities of Pol IV, Pol V, and RDR2 reveal coupling of Pol IV and RDR2 for dsRNA synthesis in plant RNA silencing. Mol. Cell **48:** 811–818.

Harris, E.Y., Ponts, N., Le Roch, K.G., and Lonardi, S. (2012). BRAT-BW: efficient and accurate mapping of bisulfite-treated reads. Bioinformatics **28:** 1795–1796.

Hazbun, T.R., et al. (2003). Assigning function to yeast proteins by integration of technologies. Mol. Cell **12:** 1353–1365.

He, X.J., Hsu, Y.F., Pontes, O., Zhu, J., Lu, J., Bressan, R.A., Pikaard, C., Wang, C.S., and Zhu, J.K. (2009a). NRPD4, a protein related to the RPB4 subunit of RNA polymerase II, is a component of RNA polymerases IV and V and is required for RNA-directed DNA methylation. Genes Dev. **23:** 318–330.

He, X.J., Hsu, Y.F., Zhu, S., Liu, H.L., Pontes, O., Zhu, J., Cui, X., Wang, C.S., and Zhu, J.K. (2009b). A conserved transcriptional regulator is required for RNA-directed DNA methylation and plant development. Genes Dev. **23:** 2717–2722.

Herr, A.J., Jensen, M.B., Dalmay, T., and Baulcombe, D.C. (2005). RNA polymerase IV directs silencing of endogenous DNA. Science **308:** 118–120.

Huang, L., Jones, A.M., Searle, I., Patel, K., Vogler, H., Hubner, N.C., and Baulcombe, D.C. (2009). An atypical RNA polymerase involved in RNA silencing shares small subunits with RNA polymerase II. Nat. Struct. Mol. Biol. **16:** 91–93.

Jeronimo, C., et al. (2004). RPAP1, a novel human RNA polymerase II-associated protein affinity purified with recombinant wild-type and mutated polymerase subunits. Mol. Cell. Biol. **24:** 7043–7058.

Kanno, T., Huettel, B., Mette, M.F., Aufsatz, W., Jaligot, E., Daxinger, L., Kreil, D.P., Matzke, M., and Matzke, A.J. (2005). Atypical RNA polymerase subunits required for RNA-directed DNA methylation. Nat. Genet. **37:** 761–765.

Kanno, T., et al. (2010). RNA-directed DNA methylation and plant development require an IWR1-type transcription factor. EMBO Rep. **11:** 65–71.

Kimura, M., Ishiguro, A., and Ishihama, A. (1997). RNA polymerase II subunits 2, 3, and 11 form a core subassembly with DNA binding activity. J. Biol. Chem. **272:** 25851–25855.

Kolodziej, P.A., and Young, R.A. (1991). Mutations in the three largest subunits of yeast RNA polymerase II that affect enzyme assembly. Mol. Cell. Biol. **11:** 4669–4678.

Lahmy, S., Guilleminot, J., Schmit, A.C., Pelletier, G., Chaboute, M.E., and Devic, M. (2007). QQT proteins colocalize with microtubules and are essential for early embryo development in Arabidopsis. Plant J. **50:** 615–626.

Langmead, B., Trapnell, C., Pop, M., and Salzberg, S.L. (2009). Ultrafast and memory-efficient alignment of short DNA sequences to the human genome. Genome Biol. **10:** R25.

Law, J.A., and Jacobsen, S.E. (2010). Establishing, maintaining and modifying DNA methylation patterns in plants and animals. Nat. Rev. Genet. **11:** 204–220.

Law, J.A., Vashisht, A.A., Wohlschlegel, J.A., and Jacobsen, S.E. (2011). SHH1, a homeodomain protein required for DNA methylation, as well as RDR2, RDM4, and chromatin remodeling factors, associate with RNA polymerase IV. PLoS Genet. **7:** e1002195.

Law, J.A., Du, J., Hale, C.J., Feng, S., Krajewski, K., Palanca, A.M., Strahl, B.D., Patel, D.J., and Jacobsen, S.E. (2013). Polymerase IV occupancy at RNA-directed DNA methylation sites requires SHH1. Nature **498:** 385–389.

Li, C.F., Pontes, O., El-Shami, M., Henderson, I.R., Bernatavichute, Y.V., Chan, S.W., Lagrange, T., Pikaard, C.S., and Jacobsen, S.E. (2006). An ARGONAUTE4-containing nuclear processing center colocalized with Cajal bodies in *Arabidopsis thaliana*. Cell **126:** 93–106.

Matzke, M., Kanno, T., Daxinger, L., Huettel, B., and Matzke, A.J. (2009). RNA-mediated chromatin-based silencing in plants. Curr. Opin. Cell Biol. **21:** 367–376.

Mi, S., et al. (2008). Sorting of small RNAs into Arabidopsis argonaute complexes is directed by the 5′ terminal nucleotide. Cell **133:** 116–127.

Minaker, S.W., Filiatrault, M.C., Ben-Aroya, S., Hieter, P., and Stirling, P.C. (2013). Biogenesis of RNA polymerases II and III requires the conserved GPN small GTPases in *Saccharomyces cerevisiae*. Genetics **193:** 853–864.

Muñoz, A., Mangano, S., González-García, M.P., Contreras, R., Sauer, M., De Rybel, B., Weijers, D., Sánchez-Serrano, J.J., Sanmartín, M., and Rojo, E. (2017). RIMA-dependent nuclear accumulation of IYO triggers auxin-irreversible cell differentiation in Arabidopsis. Plant Cell **29:** 575–588.

Niesser, J., Wagner, F.R., Kostrewa, D., Mühlbacher, W., and Cramer, P. (2015). Structure of GPN-Loop GTPase Npa3 and implications for RNA Polymerase II assembly. Mol. Cell. Biol. **36:** 820–831.

Onodera, Y., Haag, J.R., Ream, T., Costa Nunes, P., Pontes, O., and Pikaard, C.S. (2005). Plant nuclear RNA polymerase IV mediates siRNA and DNA methylation-dependent heterochromatin formation. Cell **120:** 613–622.

Pontes, O., Li, C.F., Costa Nunes, P., Haag, J., Ream, T., Vitins, A., Jacobsen, S.E., and Pikaard, C.S. (2006). The Arabidopsis chromatin-modifying nuclear siRNA pathway involves a nucleolar RNA processing center. Cell **126:** 79–92.

Pontier, D., Yahubyan, G., Vega, D., Bulski, A., Saez-Vasquez, J., Hakimi, M.A., Lerbs-Mache, S., Colot, V., and Lagrange, T. (2005). Reinforcement of silencing at transposons and highly repeated sequences requires the concerted action of two distinct RNA polymerases IV in Arabidopsis. Genes Dev. **19:** 2030–2040.

Qi, Y., Denli, A.M., and Hannon, G.J. (2005). Biochemical specialization within Arabidopsis RNA silencing pathways. Mol. Cell **19:** 421–428.

Ream, T.S., Haag, J.R., Wierzbicki, A.T., Nicora, C.D., Norbeck, A.D., Zhu, J.K., Hagen, G., Guilfoyle, T.J., Pasa-Tolić, L., and Pikaard, C.S. (2009). Subunit compositions of the RNA-silencing enzymes Pol IV and Pol V reveal their origins as specialized forms of RNA polymerase II. Mol. Cell **33:** 192–203.

Sanmartín, M., Sauer, M., Muñoz, A., Zouhar, J., Ordóñez, A., van de Ven, W.T., Caro, E., de la Paz Sánchez, M., Raikhel, N.V., Gutiérrez, C., Sánchez-Serrano, J.J., and Rojo, E. (2011). A molecular switch for initiating cell differentiation in Arabidopsis. Curr. Biol. **21:** 999–1008.

Schwab, R., Ossowski, S., Riester, M., Warthmann, N., and Weigel, D. (2006). Highly specific gene silencing by artificial microRNAs in Arabidopsis. Plant Cell **18:** 1121–1133.

Silva, J.C., Gorenstein, M.V., Li, G.Z., Vissers, J.P., and Geromanos, S.J. (2006). Absolute quantification of proteins by LCMSE: a virtue of parallel MS acquisition. Mol. Cell. Proteomics **5:** 144–156.

Staresincic, L., Walker, J., Dirac-Svejstrup, A.B., Mitter, R., and Svejstrup, J.Q. (2011). GTP-dependent binding and nuclear transport of RNA polymerase II by Npa3 protein. J. Biol. Chem. **286:** 35553–35561.

Tucker, S.L., Reece, J., Ream, T.S., and Pikaard, C.S. (2010). Evolutionary history of plant multisubunit RNA polymerases IV and V: subunit origins via genome-wide and segmental gene duplications, retrotransposition, and lineage-specific subfunctionalization. Cold Spring Harb. Symp. Quant. Biol. **75:** 285–297.

Wang, W., Ye, R., Xin, Y., Fang, X., Li, C., Shi, H., Zhou, X., and Qi, Y. (2011). An importin β protein negatively regulates microRNA activity in Arabidopsis. Plant Cell **23:** 3565–3576.

Wang, Y., and Ma, H. (2015). Step-wise and lineage-specific diversification of plant RNA polymerase genes and origin of the largest plant-specific subunits. New Phytol. **207:** 1198–1212.

Wierzbicki, A.T., Haag, J.R., and Pikaard, C.S. (2008). Noncoding transcription by RNA polymerase Pol IVb/Pol V mediates transcriptional silencing of overlapping and adjacent genes. Cell **135:** 635–648.

Wierzbicki, A.T., Ream, T.S., Haag, J.R., and Pikaard, C.S. (2009). RNA polymerase V transcription guides ARGONAUTE4 to chromatin. Nat. Genet. **41:** 630–634.

Wild, T., and Cramer, P. (2012). Biogenesis of multisubunit RNA polymerases. Trends Biochem. Sci. **37:** 99–105.

Wu, L., Zhou, H., Zhang, Q., Zhang, J., Ni, F., Liu, C., and Qi, Y. (2010). DNA methylation mediated by a microRNA pathway. Mol. Cell **38:** 465–475.

Ye, R., Wang, W., Iki, T., Liu, C., Wu, Y., Ishikawa, M., Zhou, X., and Qi, Y. (2012). Cytoplasmic assembly and selective nuclear import of Arabidopsis Argonaute4/siRNA complexes. Mol. Cell **46:** 859–870.

Ye, R., Chen, Z., Lian, B., Rowley, M.J., Xia, N., Chai, J., Li, Y., He, X.J., Wierzbicki, A.T., and Qi, Y. (2016). A Dicer-independent route for biogenesis of siRNAs that direct DNA methylation in Arabidopsis. Mol. Cell **61:** 222–235.

Yoo, S.D., Cho, Y.H., and Sheen, J. (2007). Arabidopsis mesophyll protoplasts: a versatile cell system for transient gene expression analysis. Nat. Protoc. **2:** 1565–1572.

Zhang, H., Tang, K., Wang, B., Duan, C.G., Lang, Z., and Zhu, J.K. (2014). Protocol: a beginner's guide to the analysis of RNA-directed DNA methylation in plants. Plant Methods **10:** 18.

Zheng, B., Wang, Z., Li, S., Yu, B., Liu, J.Y., and Chen, X. (2009). Intergenic transcription by RNA polymerase II coordinates Pol IV and Pol V in siRNA-directed transcriptional gene silencing in Arabidopsis. Genes Dev. **23:** 2850–2860.

Zhong, X., Du, J., Hale, C.J., Gallego-Bartolome, J., Feng, S., Vashisht, A.A., Chory, J., Wohlschlegel, J.A., Patel, D.J., and Jacobsen, S.E. (2014). Molecular mechanism of action of plant DRM de novo DNA methyltransferases. Cell **157:** 1050–1060.